Available online at www.sciencedirect.com

SciVerse ScienceDirect

Procedia - Social and Behavioral Sciences 53 (2012) 1020 – 1028

Procedia
Social and Behavioral Sciences

SIIV - 5th International Congress - Sustainability of Road Infrastructures

Study of Hydroplaning Risk on Rolling and Sliding Passenger Car

Srirangam Santosh Kumar[a,*], Kumar Anupam[b], Tom Scarpas[c], Cor Kasbergen[d]

[a]*PhD Candidate, Delft University of Technology, Stevinweg 1, Delft 2628CN, The Netherlands*
[b]*Post Doctorial Researcher, Delft University of Technology, Stevinweg 1, Delft 2628CN, The Netherlands*
[c]*Head, Program of Mechanics of Infrastructure Materials, Delft University of Technology, Stevinweg 1, Delft, 2628CN, The Netherlands*
[d] *Senior Researcher, Delft University of Technology, Stevinweg 1, Delft, 2628CN, The Netherlands*

Abstract

Hydroplaning speed is known to vary over a range of tire slipping conditions from free rolling to completely skidding. An attempt has been made to simulate two extreme conditions of hydroplaning i.e. when the tire is completely rolling (0% slip) and a completely locked tire (100% slip). ASTM standard smooth tire moving over the plane pavement surface is considered in the model. The analyses showed that the hydroplaning risk associated with the locked tire is more than the rolling tire. The modeling was carried out using the commercial finite element software package, ABAQUS.

*Keywords:*Hydroplaning; Slipping and Skidding tires; Finite element method

1. Introduction

The risk of hydroplaning exists when the speed of the vehicle is high enough to develop upward hydrodynamic

Nomenclature

LF	lift force
V_h	hydrodynamic speed
ρ	density of fluid

* Corresponding author. Tel.: +31-15-278-4167 ; fax: +31-15-278-5767 .
E-mail address: S.K.Srirangam@tudelft.nl

1877-0428 doi:10.1016/j.sbspro.2012.09.951

pressure which is equal to or higher than the tire inflation pressure. Hydroplaning of vehicles is a very important safety concern particularly during wet-weather highway operations for highway authorities and road user.

Hydroplaning speed is known to vary over a range of tire slipping conditions from free rolling to skidding. In the vehicle manoeuvres particularly on a flooded pavement surface tire rolling and sliding are two important aspects. These two aspects are very important when the hydroplaning situation prevails. When hydroplaning condition prevails, there is significant loss in braking traction and steering control which may result in fatal accidents. Past researchers [1],[2],[3],[4],[5],[6],[7] and [8] conducted extensive experimental investigations on aircrafts and automobiles to demonstrate the influence of tire skidding and rolling conditions on the susceptibility of hydroplaning. Grogger and Weiss [9] and [10] developed a numerical hydroplaning model for non-rotating and rotating tires, using the combination of general-purpose packages of fluid dynamics and in-house code of structural analysis. Seta et al. [11] had come up with a new numerical procedure for rolling tire hydroplaning. The tire was analyzed by the finite element method with Lagrangian formulation, and the fluid was analyzed by the finite volume method with Eulerian formulation. A 3-D FE model of locked smooth tire hydroplaning was presented by Ong et al. [12]. Later this model was extended to hydroplaning over grooved pavements and rib tires of passenger car and truck by various researchers [13],[14],[15],[16],[17],[18],[19],[20],[21],[22] and [23]. But this model is limited to steady state hydroplaning with non-rotating tires. Cho et al. [24] presented a 3-D patterned tire hydroplaning model for determination of braking distance for tire with different slip conditions over a smooth pavement surface. Kim and Jeong [25] presented a rotating, patterned tire hydroplaning model with different yaw angles. The present study is a complementary work to the aforementioned research analyses by computing hydroplaning speeds at completely rolling and locking conditions of the wheel. In the present numerical study, a three dimensional hydroplaning model was simulated by using the commercial FE package, ABAQUS [26].

2. Objective of Study

Joyner and Horne [27] showed that the tire slipping has a significant effect on hydroplaning susceptibility. Unfortunately, full-scale experimental studies are time consuming, manpower intensive and costly to conduct. The objective of this study is to present a systematic numerical approach to understand the effect of free rolling and skidding conditions of a passenger car tire on the flow physics pertaining to hydroplaning. In this paper an assessment phenomenon of a non-rotating and rolling tire, which moves from quasi-dry state to flooded section of a pavement and eventually to the hydroplaning state has been discussed. This can be further developed to examine the transient hydroplaning performance aspect under different water depth and tire inflating pressure operating conditions. To achieve this objective, a standard ASTM smooth-tire sub-model was integrated into a three-dimensional finite-element (FE) flow model.

3. Description of Simulation Model

3.1. Study parameters

In the present analysis, three dimensional FE model of ASTM standard smooth tire (ASTM E 524) was developed for the prediction of hydroplaning speed phenomena under full rolling and locked wheel conditions. The ASTM E 524 smooth tire [28] is a size G78-15 tube-less tire of belted bias ply construction. It has a tread width of 148.6 mm and a 393.7 mm cross-sectional tread radius. The tire has a recommended cross-section width of 212.1 mm and a recommended section height of 161.0 mm when mounted on a rim. A tire inflation pressure range of 110 to 260 kPa and a wheel load of 4800 N at three different water-film thicknesses of 5.0, 7.0 and 10.0 mm were considered for the present study. A smooth analytical rigid pavement surface is assumed for the cases presented. The analytical surface feature gives the feasibility to consider any length of the pavement under

rolling/sliding wheel conditions and also makes the whole model computationally less expensive. Two scenarios of slip ratios were considered in the present analysis namely, free rolling (0% slip) and fully skidding (100%).

3.2. Model parameters

This section presents the salient features of the three-dimensional model of dynamic hydroplaning as shown in Fig 1. In the modeling of a tire, three structural components are considered namely rim, sidewalls, and tread. The tire structure is modeled by an outer rubber tread and inner reinforcing composite layers. The tire rubber is characterized as a nearly incompressible material by a Neo-Hookean hyperelasticity formulation in the finite deformation framework. The rim is modeled as a rigid surface using rigid body constraints to maintain the constant distance between the tire center and the rim surface. The inflation pressure is applied to the inside surface of the tire. The wheel load is applied at center of the tire and acts only in the vertical direction. In the present analyses, the tire is modeled in the Lagrangian framework and the fluid part is modeled with Eulerian elements fixed in the space.

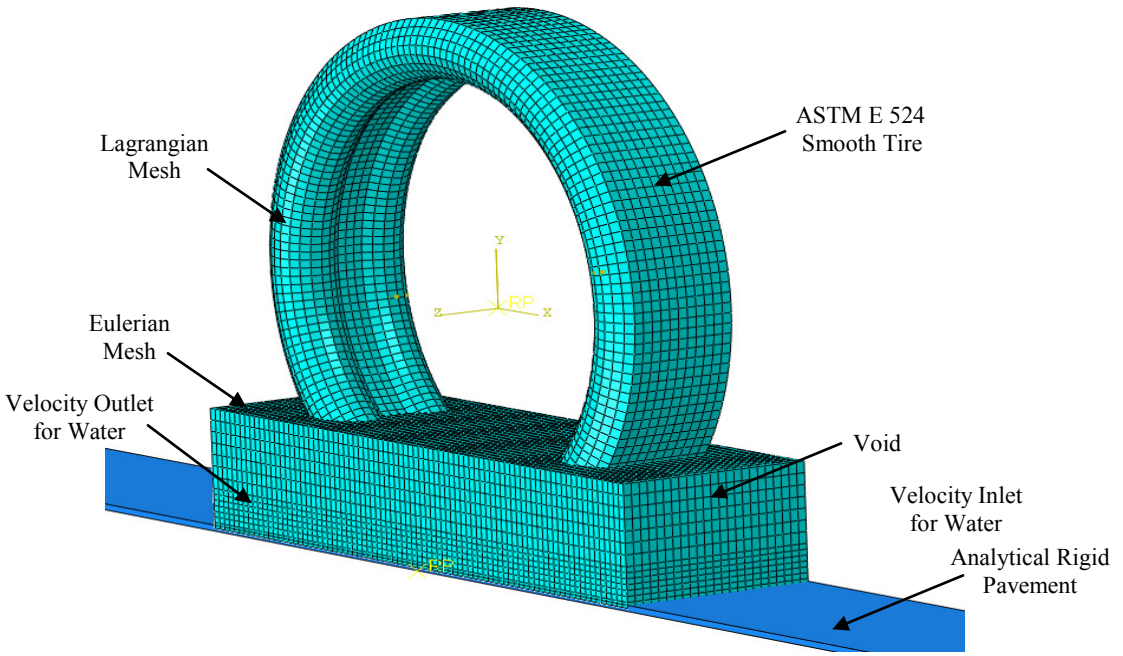

Fig. 1. proposed 3D hydroplaning model

The Lagragian and Eulerian grids are two non-matching discrete interfaces. The coupling between the Lagrangian and the Eulerian grids is enforced by imposing extra load and motion constraints. The Eulerian grid is divided into a water film layer over which another layer is modeled as a voids layer. The fluid region comprises of a velocity inlet, velocity outlet and no side flow boundary conditions. The fluid structure interaction (FSI) is modeled by using "general contact coupling algorithm" to transfer the forces between the two different frameworks. In this algorithm, Lagrangian and Eulerian equations are solved independently in the iterative partitioned approach.

The interface tracking is obtained by using the volume of fluid (VOF) method. ABAQUS [26] uses piecewise linear interface construction (PLIC) technique to calculate volume fraction of fluid in each control volume. The

Coupled Eulerian Lagrangian (CEL) algorithm considers the boundary of the Lagrangian body to identify the interface between the two different frameworks. The CEL algorithm applies the velocity of the Lagrangian body as a deformation constraint in the Eulerian calculation and the stress calculated in the Eulerian frame work is used to calculate the resulting surface stress on the Lagrangian body through contact stress constraints.

3.3. Finite element mesh design

The tire rubber is discretized using 8-node linear brick, reduced integration elements. In addition, 4 node composite shell elements are used to mesh rim. A uniform mesh distribution scheme is adopted in all regions to take care of tire rolling effect. A total of 28,628 Lagrangian 8-node hexahedron solid elements and 7,246 simplified composite shell elements for rim are used for the smooth tire. The Eulerian mesh is fixed in space unlike the Lagrangian mesh. The deformation and movement of the Lagrangian mesh causes the water to flow through the fixed Eulerian mesh elements. This results in the buildup of a high velocity and pressure gradients in the Eulerian grid. Another important observation is that a splash is formed when water strikes the tire. This demonstrates a key manifestation of the hydroplaning phenomenon, "formation of bow wave in front of tire" as shown in Fig 2. In order to capture these complex effects precisely, a fine mesh is required. The water part of Eulerian grid is made of 21,220 elements and the void region is made of 13,567 elements. It should be noted that the tire region has to be partly embedded in the Eulerian mesh. Fig 2 shows the mesh design adopted for both Lagrangian and Eulerian parts.

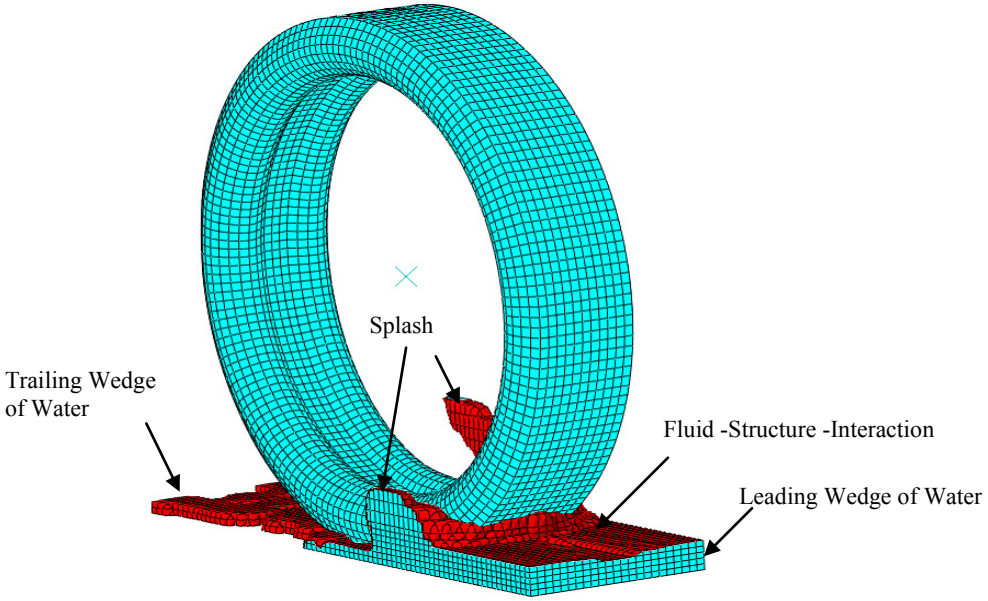

Fig. 2. ASTM E 524 smooth tire standing on water regime at the time of hydroplaning

3.4. Working mechanism of 3D hydroplaning model

The model simulation is started with tire deformation analysis under no presence of fluid by using the displacement control method. In this approach, the tire is inflated to a pre-requisite pressure, being firmly fixed at a reference position. An upward load is applied on the analytical rigid pavement which results in moving the

analytical rigid pavement towards the inflated tire and tire deformation. The static footprint of the tire is matched against the experimental results of Horne et al. [8], since accurate tire contact patch is the crucial parameter in determining accurate hydroplaning speed. Next, the analytical rigid pavement is uniformly accelerated in the horizontal direction. This forces the tire to rotate in the presence of friction until it attains a defined steady angular velocity. The same acceleration is applied to the water so that the same velocity as the analytical rigid surface is generated. In the present analysis, the hydroplaning speed is defined as the striking velocity of water at which there is no or relatively very low contact force between the tire and the analytical rigid pavement surface.

4. Validation of Simulation Model

The validation of the developed 3-dimensional hydroplaning model was made by means of the results of Horne [2, 29-30] for fully rolling and locked ASTM smooth tire. A constant water depth of 7 mm, wheel load of 4800 N and tire inflation pressure in a range of 110 kPa to 260 kPa are considered to validate the simulation model as shown in Fig 3.

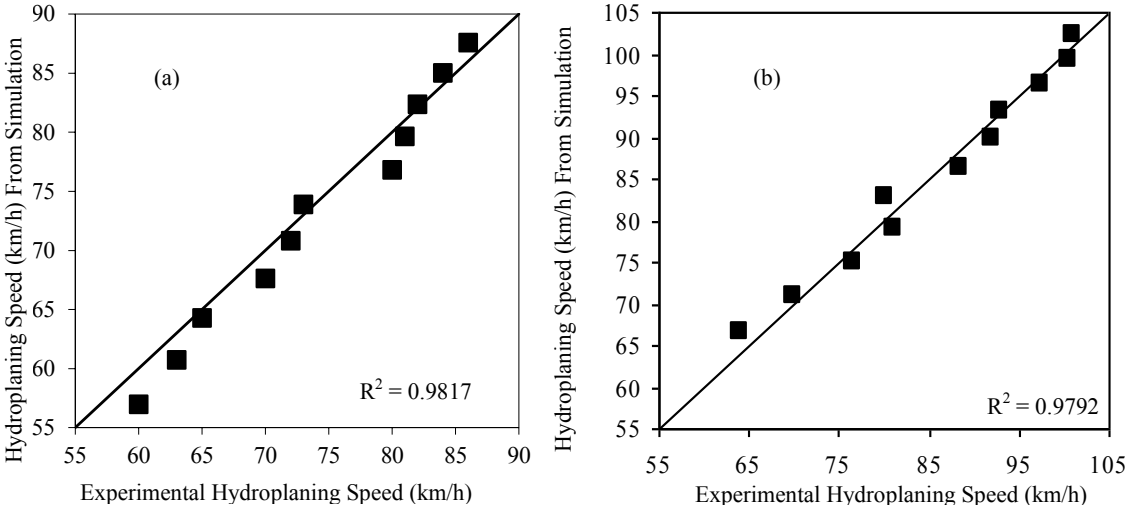

Fig. 3. verification of model for (a) sliding tire; (b) rolling tire

The pavement surface tested is considered to be a plane surface with negligible surface asperities as the flooded pavement conditions prevailed. The hydrodynamic dynamic lift generated under a tire rolling and sliding along a water-covered surface can be calculated by Equation (1) given by Horne [2],[29] and [30] with known hydrodynamic lift coefficient (C_{Lh}), tire footprint area (S) and speed (v).

$$LF = \frac{1}{2} C_{Lh} \rho v^2 S \qquad (1)$$

When total dynamic hydroplaning occurs, LF/S is equal to the tire bearing pressure that can be approximated by the tire inflation pressure (p). Hence, the total dynamic hydroplaning speed relation can be calculated as shown in Equation (2).

$$Hydroplaning\ Speed\ (V_h) = \sqrt{\frac{2p}{\mathrm{r} C_{Lh}}} \qquad (2)$$

The value of C_{Lh} is considered as 0.7 for rolling tire and 0.95 for sliding tires. These values are based on a large number of tests conducted. Using these hydrodynamic lift coefficients and the density for water, Equation (2) simplifies to Equation (3) and Equation (4).

$$V_{h,rolling} = 6.36\sqrt{p} \quad (3)$$

$$V_{h,locked} = 5.43\sqrt{p} \quad (4)$$

Fig 3 compares the measured values of hydroplaning speed based on the NASA hydroplaning equations 3 and 4, and predicted results from the simulation model. Figures show a good agreement between the experimental and the simulation model with R^2 values of 0.9817 and 0.9792 for the sliding and rolling tires respectively.

5. Analysis of Results

Fig 4 shows the plot between hydroplaning speed and tire inflation pressure for rolling and locked wheel conditions. It can be seen that the hydroplaning speed increases with the tire inflation pressure for both rolling and sliding tires, which is in agreement with the past findings by various researchers.

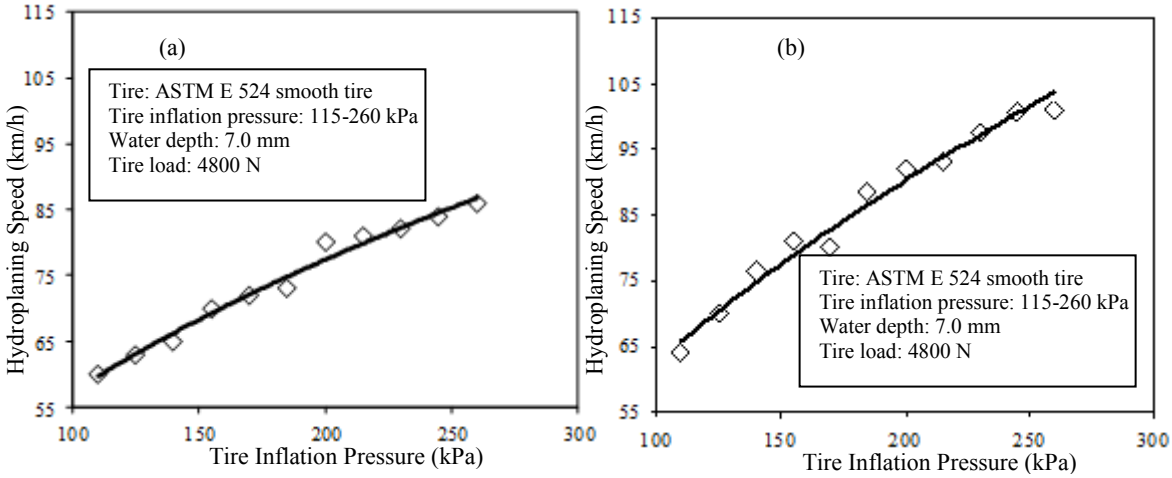

Fig 4. hydroplaning speed vs. tire inflation pressure for (a) sliding tire; (b) rolling tire

The pressure range of 110 to 155 kPa represents an under inflated tire condition which seems to be more prone to hydroplaning risk. As for instance hydroplaning speed observed at 110 kPa is reduced by 1.25 times the standard inflated case of 165.5 kPa for rolling tires. Whereas, the hydroplaning speed observed at 110 kPa is reduced by 1.18 times the standard inflated case of 165.5 kPa for sliding tires, at a constant water depth of 7 mm. A comparison between the hydroplaning risk for a free rolling tire and a sliding tire can also be observed in Fig 4. It was observed that for a free rolling case, the hydroplaning speed is about 4 km/h to 16.5 km/h higher than the fully braked tire depending upon the inflation pressure considered.

This behaviour can be attributed to the result of tire impact over the water that overcomes fluid inertia when the tire rolls on flooded pavement surface. It is believed that it is more difficult for the entrapped fluid to escape beneath a sliding tire than from a rolling tire. Fig 5 and 6 shows the variation of hydroplaning speed with tire inflation pressure at 10 mm and 5 mm respectively. Comparing the plots on Fig 4 and 5 show that the hydroplaning speed decreases with increase in water depth. It is observed that the average decrease in the

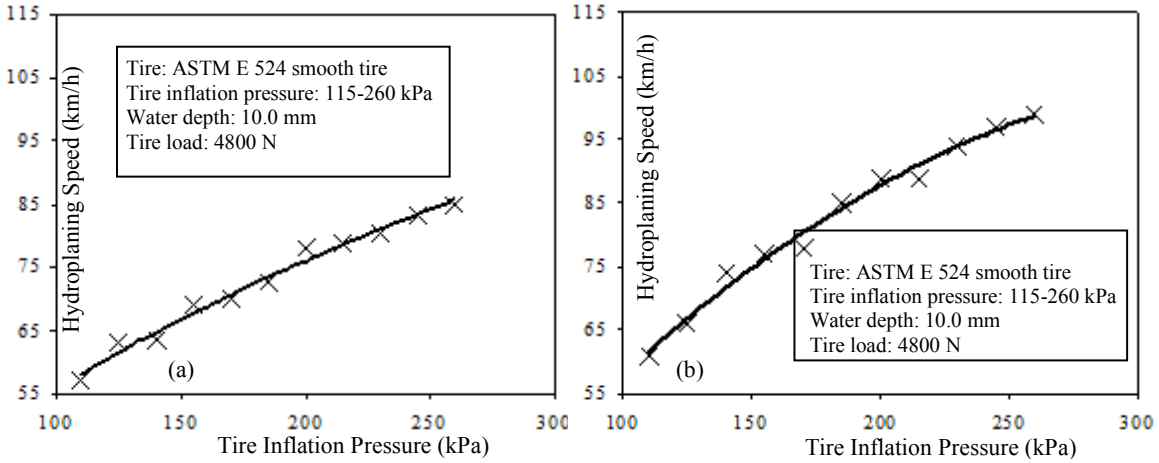

Fig 5. hydroplaning speed vs. tire inflation pressure for (a) sliding tire; (b) rolling tire

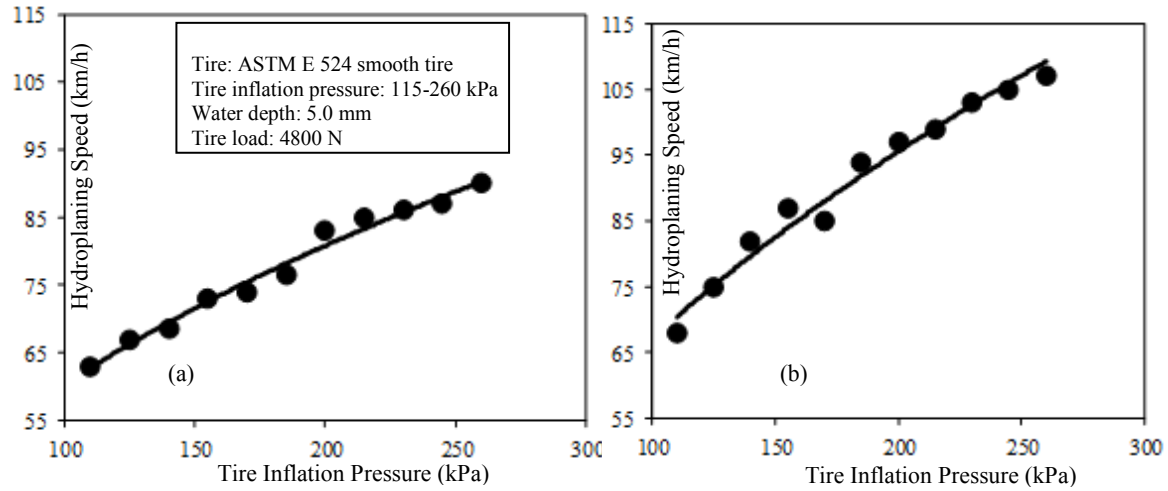

Fig 6. hydroplaning speed vs. tire inflation pressure for (a) sliding tire; (b) rolling

hydroplaning speed for a sliding tire is about 5 km/h and for a rolling tire is about 8.5 km/h with an increase of 5 mm water depth. Similar comparison can be made between Fig 4 and 6 which shows that the hydroplaning speed increases with decrease in water depth. The average increase in hydroplaning speed for a sliding tire is 3 km/h for a sliding tire and 5 km/h for a rolling tire with a decrease in water depth of 2 mm.

6. Conclusions

This study presents the development of a 3-D hydroplaning simulation model using FE tool package ABAQUS. In this study, ASTM E 524 smooth tire was considered to roll and slide over plane pavement surface. Hydroplaning speed calculated using the developed simulation model was duly validated against the past experimental studies and the results show a good agreement with the experimental findings for both rolling and

sliding cases. The simulation results also show a good agreement with the well-known NASA hydroplaning equation.

The developed model was simulated for a range of tire inflation pressure and water depth conditions. It was observed in general that the hydroplaning speed increases with the increase in tire inflation pressure for both rolling and sliding tires. In agreement with the past findings by various reseachers, it was also observed that underinflated tires and pavement with deeper water depths are more prone to the risk of hydroplaning.

When the simulation results were compared for rolling and sliding (i.e. braked wheel) tires, it was observed that sliding tires are more prone to risk of hydroplaning as compared to rolling tires because it is more difficult for the entrapped water to escape beneath a sliding tire than beneath a rolling tire. Overall, this paper shows that the presented model is a good tool to study the risk of hydroplaning for rolling and sliding tires at various operating conditions.

7. Future Developments and Recommendations

This research focuses primarily on modeling hydroplaning for locked and rolling tires. The developed model can be efficiently extended for the determination of hydroplaning speed and skid resistance for tires rolling/skidding over real pavement surface meshes. The developed model can also be extended to model hydroplaning and ski resistance under different slip and yaw conditions of tire. These applications will help highway safety authorities to assess the skid resistance and the propensity of hydroplaning associated with pavements with different asphalt mix designs under different operating conditions of vehicles.

Acknowledgements

This study was carried out in the context of the project Enhanced Driver Safety due to Improved Skid Resistance (SKIDSAFE), financed by the European Union Seventh Framework Program, Theme: Safety and Security by Design.

References

[1] Horne, W. B., & Leland, T. J. W. (1962). Influence of tire tread pattern and runway surface condition on braking friction and rolling resistance of a modern aircraft tire, NASA, TN D-1376.

[2] Horne, W. B., & Dreher, R. C. (1963). Phenomena of pneumatic tire hydroplaning, NASA, TN D-2056.

[3] Horne, W. B. (1964). Air jets a possible solution to hydroplaning and other associated runway wetness problems, Proceedings of 17th Annual International Air Safety Seminar, flight Safety foundation, New York City.

[4] Horne, W. B., & Joyner, U. T. (1965). Pneumatic tire hydroplaning and some effects on vehicle performance, SAE International Automotive Engineering Congress, Detroit, Michigan.

[5] Horne, W. B. (1968). Tire hydroplaning and its effects on tire traction, Transportation Research Board, Highway Research Record, 214, 24-33.

[6] Horne, W.B. (1969). Pavement grooving and traction studies. results from studies of highway grooving and texturing at NASA wallops station, NASA SP-5073, 425-464.

[7] Horne, W.B., & Buhlmann, F. (1983). A method for rating the skid resistance and micro/macrotexture characteristics of wet pavements, Frictional Interaction of Tire and Pavement, ASTM STP 793.

[8] Horne, W. B., Yager, T. J., & Ivey, D. L. (1986). Recent studies to investigate effects of tire footprint aspect ratio on dynamic hydroplaning speed, The Tire Pavement Interface, ASTM STP 929, 26-46.

[9] Grogger, H., & Weiss, M. (1996). Calculation of the three-dimensional free surface flow around an automobile tire, Tire Science and Technology, 24, 39.

[10] Grogger, H., & Weiss, M. (1997). Calculation of hydroplaning of a deformable smooth-shaped and longitudinally-grooved tire, Tire Science and Technology, 25, 265.

[11] Seta, E. (2000). Hydroplaning analysis by FEM and FVM: effect of tire rolling and tire pattern on hydroplaning, JSAE, Japan,1, 44.
[12] Ong, G. P., Fwa, T. F., & Guo, J. (2005). Modeling hydroplaning and effects of pavement microtexture, Transportation Research Record: Journal of the Transportation Research Board, 1905/2005, 166-176.
[13] Ong, G. P., & Fwa, T. F.(2005). Analysis of effectiveness of longitudinal grooving against hydroplaning , TRB 2006 Annual Meeting.
[14] Ong, G. P., & Fwa, T. F. (2006). Transverse pavement grooving against hydroplaning I: simulation model, J. Transp. Eng., 132 (6), 10.1061/(ASCE)0733-947X(2006)132:6(441), 441–448.
[15] Ong, G. P., & Fwa, T. F. (2007). Modeling wet tire-pavement interaction: Model development, J. Transp. Eng., No. 133 (10), 10.1061/(ASCE)0733-947X(2007)133:10(590), 590–598.
[16] Ong, G. P., & Fwa, T. F. (2007). Wet-pavement hydroplaning risk and skid resistance: modeling, J. Transp. Eng. , No. 133 (10), 590–598.
[17] Ong, G.P., & Fwa, T. F. (2007). Prediction of wet-pavement skid resistance and hydroplaning potential, Transportation Research Record, 2005, 160–171.
[18] Ong, G. P., & Fwa, T. F. (2010). Modeling skid resistance of commercial trucks on highways, J. Transp. Eng., No.136 (6), 510–517.
[19] Fwa,T.F.,& Ong,G.P.(2006).Transverse pavement grooving against hydroplaning II: Design, J. Transp. Eng., No.132 (6),10.1061/(ASCE)0733-947X(2006)132:6(449), 449–457.
[20] Fwa, T. F. , Kumar, S. S. , Anupam, K., & Ong, G. P. (2009). Effectiveness of tire-tread patterns in reducing the risk of hydroplaning , J. Transp. Res. Board , No. 2094 (-1),10.3141/2094-10, 91–102.
[21] Fwa, T., Pasindu, H., & Ong, G.P. (2012). Critical rut depth for pavement maintenance based on vehicle skidding and hydroplaning consideration., J. Transp. Eng., No. 138(4), 10.1061/(ASCE)TE.1943-5436.0000336, 423–429.
[22] Kumar, A., Fwa, T. F., & Ong, G.P. (2009). Pavement grooving and vehicle hydroplaning, Transportation Research Board Annual Meeting , Paper No. 09-1181.
[23] Pasindu, H. R.. , Fwa, T. F., & Ong, G. P. (2011). Computation of aircraft braking distances , TRB 2011 Annual Meeting.
[24] Cho, J. R.., Lee, H. W., Sohn, J. S., Kim, G. J., & Woo, J. S. (2006). Numerical investigation of hydroplaning characteristics of three-dimensional patterned tire, European Journal of Mechanics A/Solids, 914-926.
[25] Kim, T.W., & Jeong, H.Y. (2010). Hydroplaning simulations for tires using FEM, FVM and an asymptotic method, International Journal Of Automotive Technology, Volume 11, DOI: 10.1007/s12239-010-0107-0, 901-908.
[26] ABAQUS.(2010).Version 6.10 User's Manual, Hibbit, Karlson & Sorensen, Inc.
[27] Joyner, U.T., and Horne, W.B. (1971). Determining causation of aircraft skidding accidents or incidents, Annual Corp. Aircraft Safety Seminar, Washington D.C.
[28] ASTM Standard E 524-88. (2006). Standard Specification for Standard Smooth Tire for Pavement Skid-Resistance Tests, ASTM Standards Sources (CD-ROM), ASTM, Philadelphia.
[29] Horne, W.B. (1975). Wet runways, NASA TM X-72650.
[30] Horne, W.B. (1976). Status of runway slipperiness, NASA SP-416, 191-245.